Hindered Rotation Leading to Nonequivalence in 2-Substituted Benzyl Cobaloximes: Structure−Property Relationship†

Debaprasad Mandal and B. D. Gupta*

Department of Chemistry, Indian Institute of Technology, Kanpur, India 208016

Received October 12, 2006

Benzyl cobaloximes with substituents at the 2-position having varying electronic and steric properties have been synthesized and characterized. Three different dioximes (dmgH, dpgH, gH) have been used. The dmgH(Me) and Co-bound CH_2 protons show nonequivalence in the ^{1}H NMR at subzero temperatures. The nonequivalence has been rationalized in terms of restricted rotation of the Co−C and/or C−Ph bond and is attributed to weak interactions between axial and equatorial ligands. T_c depends upon the nature of the 2-substituent and the dioxime. The molecular structures of 2-Me-$C_6H_4CH_2Co(dmgH)_2Py$, 2-naphthyl-$CH_2Co(dmgH)_2Py$, 2-Br-$C_6H_4CH_2Co(gH)_2Py$, and $C_6H_5CH_2Co(dpgH)_2Py$ are reported. The activation energies of Co−C and C−Ph bond rotation are calculated from variable-temperature ^{1}H NMR data using line-shape analysis. Also, the theoretical calculations using DFT are performed on 2-Me-$C_6H_4CH_2Co(dmgH)_2Py$ and 2-Br-$C_6H_4CH_2Co(gH)_2Py$ for the Co−C and C−Ph bond rotation. The conformational energy diagrams of these two molecules have been discussed.

Introduction

The unique property of coenzyme B_{12} arises from the different catalytic activity of two different coenzymes. How the Co−C bond is activated toward homolysis or heterolysis is an enduring subject of research.[1] Recently it was revealed that the Co−C bond cleavage is not the rate-determining step.[2] The destabilization is due to the interaction of substrate with the coenzyme. The maximum distortion found is in the ribose moiety during the Co−C bond rupture, while the adenine moiety is stabilized due to its interaction with the corrin side chain and the enzyme.[2]

Organocobaloximes, $RCo(dmgH)_2Py$, have extensively been used to mimic the B_{12} coenzyme, and studies have continued to complement those on the more complex cobalamin and B_{12}-based proteins. Solution studies on alkylcobalamins and organocobaloximes suggest that the Co−C bond length is responsive to both steric and electronic effects in organocobalt(III) compounds.[3]

Schrauzer et al.[4] made an observation in 1981 that benzyl cobalamin undergoes decomposition faster than bulky neopentyl in solution and it is not solely due to steric reasons; there is some additional force that makes the benzyl−Co bond weaker. The studies in model compounds have also shown that the benzyl cobaloximes behave differently from alkyl cobaloximes. The difference in reactivity must be due to some interactions of the benzyl group with the dioxime, and such interactions must be lacking in the alkyl group.[5]

Most of the recent studies have focused on the spectral and structural properties of cobaloximes, and NMR, in particular, has been extensively used for this purpose.[6,7] In the majority of the cobaloxime complexes, the dmgH methyl signal appears as a sharp singlet at around 2.0 ppm in the ^{1}H NMR spectra, indicating the chemical equivalence of all four methyl groups. A singlet is also expected on the basis of the mean C_{2v} symmetry of the cobaloxime and fast rotation of the Co−C bond, faster than the NMR time scale.

Nonequivalence of the dmgH methyl, however, has been observed in a few cases when either of the axial ligands is chiral: $Me(CN)CHCo(dmgH)_2Py$ and $MeCo(dmgH)_2NH(Me)CH_2Ph$).[8] A fast rotation of the Co−C bond produces two sets of diastereomers to show the dmgH methyls at a 1:1 ratio. Recently, a few complexes have shown the nonequivalence of the dmgH(Me) protons; for example, the nonequivalence results from the hindered rotation of the axial 2-aminopyridine ligand in $CF_3CH_2Co(dmgH)_2(2\text{-}NH_2Py)$, caused by H-bonding of the NH_2 group to O−H···O bridges of the dmgH ligand.[9] Similarly a hindered rotation of the 2-fluorocyclohexyl group around the Co−C bond in 2-fluorocycloalkylcobaloxime causes nonequivalence and the dmgH methyl appears as two signals in a 1:1 ratio.[10]

The nonequivalence of the dmgH methyl in organobridged dicobaloximes of the type $PyCo(dmgH)_2$-[*ortho* (and *meta*)-xylylene]-$Co(dmgH)_2Py$ has also been observed.[11] This is the

* Corresponding author. Tel: +91-512-2597046. Fax: +91-512-2597436. E-mail: bdg@iitk.ac.in.

† Dedicated to Dr. T. Ramasamy, DST, New Delhi, India.

(1) (a) Brown, K. L. *Dalton Trans.* **2006**, 1123. (b) Randaccio, L. *Comments Inorg. Chem.* **1999**, *21*, 327.

(2) Jensen, K. P.; Ryde, U. *J. Am. Chem. Soc.* **2005**, *127*, 9117.

(3) Bresciani-Pahor, N.; Forcolin, M.; Marzilli, L. G.; Randaccio, L.; Summers, M. F.; Toscano, P. J. *Coord. Chem. Rev.* **1985**, *63*, 1.

(4) Schrauzer, G. N.; Grate, J. H. *J. Am. Chem. Soc.* **1981**, *103*, 541.

(5) (a) Toscano, P. J.; Brand, H.; Liu, S.; Zubieta, J. *Inorg. Chem.* **1990**, *29*, 2101. (b) Ng, F. T. T.; Rempel, G. L.; Mancuso, C.; Halpern, J. *Organometallics* **1990**, *9*, 2762. (c) Brown, T. M.; Cooksey, C. J.; Dronsfield, A. T.; Fowler, J. H. *Inorg. Chim. Acta* **1999**, *288*, 112. (d) Brown, T. M.; Dronsfield, A. T.; Wilkinson, A. S. *Inorg. Chim. Acta* **1997**, *262*, 97. (e) Daikh, B. E.; Finke, R. G. *J. Am. Chem. Soc.* **1992**, *114*, 2938.

(6) (a) Bresciani-Pahor, N.; Geremia, S.; López, C.; Randaccio, L.; Zangrando, E. *Inorg. Chem.* **1990**, *29*, 1043. (b) Toscano, P. J.; Marzilli, L. G. *Prog. Inorg. Chem.* **1985**, *31*, 105. (c) Gilaberte, J. M.; López, C.; Alvarez, S.; Font-Altaba, M.; Solans, X. *New J. Chem.* **1993**, *17*, 193. (d) López, C.; Alvarez, S.; Solans, X.; Font-Altaba, M. *Inorg. Chim. Acta* **1986**, *111*, L19.

(7) Mandal, D.; Gupta, B. D. *Organometallics* **2005**, *24*, 1501.

(8) (a) Clifford, B.; Cullen, W. R. *J. Chem. Educ.* **1983**, *60*, 555. (b) Naumberg, M.; Duong, K. N. V.; Gaudemer, F.; Gaudemer, A. *C. R. Acad. Sci., Ser. C* **1970**, *270*, 1301. (c) Cabaret, D.; Maigrot, N.; Welvart, Z.; Duong, K. N. V.; Gaudemer, A. *J. Am. Chem. Soc.* **1984**, *106*, 2870.

(9) Marzilli, L. G.; Summers, M. F.; Zangrando, E.; Bresciani-Pahor, N.; Randaccio, L. *J. Am. Chem. Soc.* **1986**, *108*, 4830.

(10) Galinkina, J.; Rusanov, E.; Wagner, C.; Schmidt, H.; Ströhl, D.; Tobisch, S.; Steinborn, D. *Organometallics* **2003**, *22*, 4873.

10.1021/om060940d CCC: $37.00
Publication on Web 01/05/2007

Scheme 1. Cobaloximes under Consideration

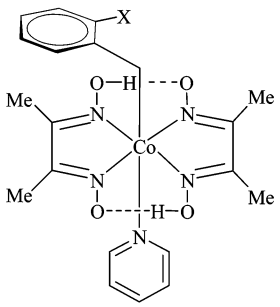

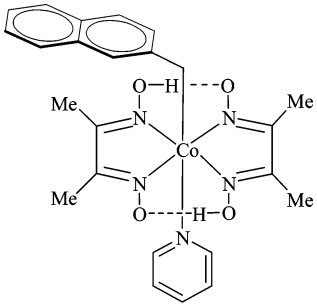

X = H, F, Cl, Br, I, CN, NO_2, Ph, CH_3, OMe (**1–10**)

2-X-$C_6H_4CH_2Co(L)_2Py$ (**1a–10a**); L= dmgH

2-X-$C_6H_4CH_2Co(L)_2Py$ (**1b–10b**); L = dpgH

2-X-$C_6H_4CH_2Co(L)_2Py$ (**1c–10c**); L = gH

2-Naphthyl-$CH_2Co(L)_2Py$

(**11a**) L = dmgH;

(**11b**) L = dpgH;

(**11c**) L = gH

first example where the cobalt-bound CH_2 behaves as diastereotopic and appears as a doublet of doublets at the freezing (lower) temperature. In the absence of crystal structure it was assumed that the bulkiness of two cobaloxime units caused the hindered rotation. Later, the crystal structure of 2-NO_2-C_6H_3-$[CH_2Co(dmgH)_2Py]_2$ showed that the bulkiness was similar to simple benzyl cobaloxime, $BnCo(dmgH)_2Py$,[12] and the benzyl group was oriented in such a way that it lay over one of the dioxime wings, as seen earlier in many of the crystal structures of benzyl cobaloximes.[13,14] This has posed another question: whether the π-interaction between the benzyl group and the dioxime ring current[6d,7] contributes to the nonequivalence of the dmgH(Me) in some way.

In a recent communication we have shown that the ^{1}H NMR spectrum of benzyl cobaloxime in $CDCl_3$ shows a 12H singlet for the dmgH(Me) at 1.95 ppm even at −55 °C,[11] but it appears as two singlets (1:1) in 2-Br-$C_6H_4CH_2Co(dmgH)_2Py$ at −50 °C.[14] Also, the cobalt-bound CH_2 splits at −14 °C and appears as a doublet of doublets at lower temperature. A similar observation is made in 2-Me-$C_6H_4CH_2Co(dmgH)_2Py$, but the coalescence temperature for the dmgH(Me) is higher (−20 °C) as compared to CH_2 (−45 °C). We have proposed that the weak π-interactions in 2-substituted benzyl cobaloximes cause the restriction of the Co−C and/or C−Ph bond rotation and are responsible for the nonequivalence of dmgH(Me) and CH_2 protons in ^{1}H NMR.[14]

Since the nonequivalence of dmgH(Me) and CH_2 protons occurs at different temperatures, it is quite possible that two different processes are taking place and these may have the same/different origins. If the weak π-interaction is important, as the preliminary results show, the nonequivalence of the dmgH or CH_2 groups will occur irrespective of the nature of dioxime and the extent of nonequivalence will depend on the ring current and puckering of the dioxime. The process of nonequivalence appears more complicated than what was assumed initially.

The other important questions at this stage are as follows: what is the origin of hindered rotation of the Co−C or C−Ph bond? Is there any conclusive evidence to show that the hindered rotation is partly due to an interaction of aromatic ring π-electrons with the dioxime ring current? What is the role of the 2-substituent; does it have any direct interaction with the dioxime or CH_2 protons or does it simply affect the electron density in the phenyl ring?

In order to rationalize the above questions and to see the role of the 2-substituent, we have undertaken ^{1}H NMR studies in 2-X-$C_6H_4CH_2Co(dioxime)_2Py$. Here the substituent X has been chosen such that it varies in steric size and in electron donation/withdrawal capacity (Scheme 1).

Results and Discussion

Spectroscopy: Characterization. ^{1}H NMR. All the complexes (**1**−**11a**,**b**,**c**) are primarily characterized by ^{1}H and ^{13}C NMR spectroscopy, and the data are shown in Tables 1 (^{1}H) and S2 (^{13}C, Supporting Information). The ^{1}H and ^{13}C NMR spectra are easily assigned on the basis of the chemical shifts. The peaks are assigned according to their relative intensities and are consistent with the related dioxime complexes previously described.[15]

Dioxime. 1−**11a.** The dmgH methyl protons appear as a singlet between 1.80 and 2.07 ppm, and the upfield shift follows the order when X is CN < F ≈ Cl ≈ Br ≈ I ≈ NO_2 < H ≈ OMe < CH_3 < Ph < 2-Naph.

1−**11b.** It has not been possible to distinguish between dpgH and benzyl protons.

1−**11c.** gH protons appear between 7.24 and 7.38 ppm, and the upfield shift follows the order CN ≈ Ph < F ≈ Cl ≈ Br ≈ I ≈ NO_2 < H ≈ OMe ≈ CH_3 < 2-Naph.

In general, the dioxime protons appear upfield in benzyl cobaloximes as compared to the alkyl analogues.[15,16] This might be due to the interaction of the benzyl group with the dioxime. The upfield shift order of the dioxime protons in dmgH or gH complexes clearly indicates that the ring current effect of the benzyl group depends on the 2-substituent. Although the chemical shift difference does not appear to be that large, it is significant in view of the reports by López et al., who have listed the ligands on the basis of small chemical shift difference (<0.05 ppm).[17] Among the entire series the 2-CN derivative

(11) Gupta, B. D.; Vijaikanth, V.; Singh, V. *Organometallics* **2004**, *23*, 2069.

(12) Vijaikanth, V.; Gupta, B. D.; Mandal, D.; Shekhar, S. *Organometallics* **2005**, *24*, 4454.

(13) (a) Bresciani-Pahor, N.; Randaccio, L.; Zangrando, E. *Acta Crystallogr. Sect. C* **1988**, *44*, 2052. (b) Tyrlik, S. K.; Lenstra, A. T. H.; Van Loock, J. F. J.; Geise, H. J.; Dommisse, R. A. *Acta Crystallogr. Sect. C* **1986**, *42*, 553. (c) Cesario, M.; Giannotti, C.; Guilhem, J.; Zakrzewski, J. *Acta Crystallogr. Sect. C* **1992**, *48*, 798. (e) Domingo, M. R.; Irving, A.; Liao, Y.; Moss, J. R.; Nash, A. *J. Orgnomet. Chem.* **1993**, *443*, 232. (d) Gupta, B. D.; Yamuna, R.; Singh, V.; Tiwari, U.; Barclay, T.; Cordes, W. *J. Organomet. Chem.* **2001**, *627*, 80.

(14) Mandal, D.; Gupta, B. D. *Organometallics* **2006**, *25*, 3305.

(15) Gupta, B. D.; Vijaikanth, V.; Singh, V. *J. Organomet. Chem.* **1998**, *570*, 1.

(16) Gupta, B. D.; Qanungo, K. *J. Organomet. Chem.* **1997**, *543*, 125.

Table 1. ^{1}H NMR Data for (1−11)a−c at Room Temperature in $CDCl_3$

				pyridine			
no.	O-H···O	CH_2−Co	dmgH/dpgH/gH	α (d)	β (t)	γ (t)	aromatic/others
1a	18.30	2.85	1.95	8.54	7.27	7.68	6.97−7.02(m), 7.10−7.13(m)
2a	18.25	2.79	2.00	8.53	7.28	7.68	6.73−6.82(m), 6.98(t), 7.07−7.09(m)
3a	18.23	2.94	2.01	8.54	7.28	7.68	6.91−6.94(m), 7.03−7.07(m)
4a	18.26	2.96	2.02	8.53	7.27	7.68	6.96−6.98(m), 7.04−7.06(m), 7.26(d)
5a	18.24	2.97	2.02	8.53	7.28	7.68	6.77−6.81(m), 6.96−7.06(m), 7.56(d)
6a	18.16	2.85	2.07	8.49	7.28	7.69	7.02−7.05(m), 7.17−7.23, 7.26−7.33(m)
7a	18.08	3.23	2.02	8.43	7.26	7.67	6.99−7.01(m), 7.15−7.27(m), 7.73(m)
8a	17.90	3.15	1.88	8.41	7.19	7.61	6.82−7.07(m), 7.30−7.48(m)
9a	18.37	2.92	1.93	8.52	7.26	7.65	6.79(d), 6.86(d), 7.03(m), 2.08 (CH_3)
10a	18.24	2.96	1.96	8.57	7.26	7.66	6.56−6.61(m), 6.85(d), 7.12(t), 3.75(s, OCH_3)
11a	18.34	3.01	1.84	8.55	*b*	*b*	7.15(d), 7.25−7.39(m), 7.48(d), 7.65(t), 7.65(t)
1b	18.73	3.44	*b*	8.86	7.40	7.79	6.93(d), 7.11−7.27(m), 7.34(d)
2b	18.57	*c*	*b*	8.78		7.79	6.76−7.39
3b	18.64	3.55[a]	*b*	8.81	7.43	7.85	6.79−7.26
4b	18.44	3.57[a]	*b*	8.83	7.46	7.89	7.11−7.30
5b	18.52	3.57[a]	*b*	8.82	7.46	7.88	6.82−7.32
6b	18.71	3.50	*b*	8.80	7.40	7.81	7.00−7.27
7b	18.63	*c*	*b*	8.68	7.37	7.83	7.01−7.29
8b	18.46	3.72	*b*	8.72	*b*	7.73	6.82(d), 7.00(t), 7.13−7.21, 7.31(t), 7.36−7.44(m), 7.57(d)
9b	18.82	*c*	*b*	8.87	*b*	7.82	6.91−7.41, 2.08 (CH_3)
10b	18.65	3.62	*b*	8.81	7.33	7.72	6.72−7.73, 3.74 (OCH_3)
11b	18.79	3.61	*b*	8.85	7.38	7.81	6.80−7.93
1c	17.67	3.01	7.24	8.54	7.35	7.75	7.11−7.05(m)
2c	17.59	2.97	7.29	8.53	7.34	7.75	7.03−7.18(m), 6.77−6.85(m)
3c	17.68	3.13	7.31	8.54	7.34	7.75	7.09−7.17(m), 6.95−6.99(m)
4c	17.69	3.14	7.32	8.53	7.35	7.75	7.18−7.20(m), 7.01−7.04(m)
5c	17.54	3.03	7.28	8.44	*b*	7.76	6.76−7.20, 7.78−7.51
6c	17.47	3.05	7.38	8.49	*b*	7.78	7.24−7.24(m), 7.33−7.38(m)
7c	17.42	3.43	7.30	8.43	7.33	7.72	7.17(d), 7.23−7.30(m)
8c	17.32	3.40	7.38	8.38	b	7.67	7.03−7.09(m), 7.22−7.57(m)
9c	17.81	3.14	7.24	8.56	7.35	7.75	6.87−6.94(m), 7.03(d), 7.10(t), 2.14(CH_3)
10c	17.47	3.17	7.24	8.57	7.33	7.74	6.60−6.67(m), 6.98−7.03(m), 7.16−7.24(m), 3.76(s, OCH_3)
11c	17.74	3.18	7.21	8.55	7.34	7.75	7.40−7.69(m)

[a] Broad peak. [b] Merge with aromatic protons. [c] Not observed.

(**6**) shows the lowest chemical shift. The orientation of the 2-Ph group affects the chemical shift in **8**, and this is similar to our observation in the reported biphenyl-substituted mono- or dicobaloximes.[11] To summarize, it is the total electron density in the benzyl group that interacts with the dioxime protons, the 2-substituent contributes to this electron density, and the chemical shift of dioxime protons follows the electronic effect of the 2-substituent.

CH_2. The cobalt-bound methylene protons always appear as a broad singlet at room temperature in most of the complexes. In some of the dpgH complexes the CH_2−Co peak is not visible; the same was observed earlier in the xylylene-bridged dicobaloximes.[11,12]

The following chemical shift order is observed.

1−11a: F > 2-Naph ≈ H ≈ CN > CH_3 ≈ OMe ≈ Cl ≈ Br ≈ I > NO_2 ≈ Ph.

1−11b: H > CN > Cl ≈ Br ≈ I > OMe > Ph > 2-Naph.

1−11c: F ≈ H ≈ I ≈ CN > Cl ≈ Br ≈ CH_3 ≈ OMe > 2-Naph > NO_2 ≈ Ph.

The high upfield shift in 2-F is quite surprising, and it is difficult to give any proper explanation. The chemical shift difference ($\Delta\delta$)[18] is more prominent in the dpgH and gH complexes as compared to dmgH. Interestingly, a comparison of data with the reported 4-X-$C_6H_4CH_2Co(dioxime)_2Py$ complexes shows that the shifts are much more pronounced in the 2-substituted analogues.[15] This may suggest a direct interaction of X with one of the CH_2 protons, but the extent of interaction will depend upon the orientation of the X group with respect to CH_2. This is much more conspicuous in 2-Ph, 2-NO_2 complexes. The nonequivalence of CH_2 protons however is not observed at room temperature since the average chemical shift is due to rapid oscillation around the C−Ph bond. The chemical shift of Co−CH_2 does not follow the electronic effect of the 2-substituent, as was found in dioxime protons, and unlike the dioxime protons, the nonequivalence of CH_2 should depend upon electronic effects, steric effects, and the orientation (see correlations later). The low-temperature NMR and X-ray studies give a much better picture.

Variable-Temperature ^{1}H NMR Studies. The important observations so far have been (a) without an asymmetric center

(17) (a) Gilaberte, J. M.; López, C.; Alvarez, S.; Font-Bardia, M.; Solans, X. *New J. Chem.* **1993**, *17*, 193. (b) López, C.; Alvarez, S.; Solans, X.; Font-Altaba, M. *Inorg. Chem.* **1986**, *25*, 2962.

(18) Coordination shift $\Delta\delta = (\delta_{complex} - \delta_{free\ base})$.

Table 2. σ_o, F, T_c, and $\Delta\delta$ Values[a]

	H (**1a**)	F (**2a**)	Br (**4a**)	Ph (**8a**)	CH_3 (**9a**)	OMe (**10a**)	Naph (**11a**)	Br-gH (**4c**)	Br (dm)(dp) (**4ab**)[b]
σ_o	0.00	0.29	0.55	0.21	−0.15	−0.37			
F	0.00	0.43	0.44	0.08	−0.04	0.26			
					dmgH(Me)				
T_c (°C)	−90	−50	−50	−25	−20	−20	−23		
$\Delta\delta$ (Hz)	2.40	7.2	13.6	56.0	73.5	60.5	90		
					CH_2Co				
T_c (°C)	−90	−7	−14	−15	−45	+2	−30	−23	−12
$\Delta\delta$ (Hz)	1.16	268.6	255.8	128.7	9.2	252.4	33	330.8	208.8

[a] σ_o = Taft's *ortho*-substituent constant; F = Swain and Lupton field parameter; T_c = coalescence temperature (°C); $\Delta\delta$ = difference between the two peaks at low temperature (−60 °C). [b] **4ab** = 2-Br-$C_6H_4CH_2$Co(dmgH)(dpgH)Py.

the nonequivalence of CH_2 or dmgH is observed only when the axial organic group has an aromatic ring, be it 2-substituted benzyl cobaloximes or xylylene-bridged dicobaloximes, (b) the nonequivalence has been achieved at subzero temperature, (c) the hindered rotation of the C−Ph and/or Co−C bond causes the nonequivalence, (d) π-interactions between the axial and equatorial dioxime ligand play an important role, (e) the 2-substituent alters the electron density in the aromatic ring and a direct interaction with the dioxime is also possible to influence the nonequivalence.

We still seek the answers to important questions such as (a) is it possible to distinguish between the C−Ph and Co−C bond rotation restriction processes? (b) how does the activation energy of Co−C/C−Ph bond rotation depend upon the 2-substituent? and (c) what is the relative contribution of the 2-substituent in terms of steric and electronic effect?

The nonequivalence of dioxime protons is easier to study in the dmgH complexes as compared to the complexes with other dioximes. For example, in the dpgH and gH complexes, the dioxime protons merge with the aromatic protons of the axial groups. Hence the low-temperature work has been carried out mainly in the dmgH complexes.

Variable-temperature ^{1}H NMR spectra have been recorded for **2a**, **4a**, **8a**, **9a**, **10a**, **11a**, and **4c** in the range +20 to −60 °C (Table 2). The following resonances are considered for study: (a) O−H···O, (b) pyridine, (c) CH_2, and (d) dioxime methyl.

The O−H···O peak appears as a broad singlet, Py_α as a doublet, and Py_β and Py_γ protons as triplets at all temperatures. The broad singlet for the O−H···O proton sharpens due to the slowing of the exchange rate of the oxime proton as the temperature is lowered and also it is shifted downfield. The downfield shift is 0.06 ppm for every 10 °C lowering in temperature.

To rationalize the nonequivalence in dioxime and CH_2 protons, we have considered the following possibilities.

(1) *Rotation about the Co−C bond is slowed while rotation about the C−Ph bond is still fast.* (a) If the C−Ph bond is aligned along a mirror plane as in Scheme 2a or at right angles along the other mirror plane, or the alignment is averaged along one of these planes by rapid oscillation, then the methyl signals will be split into two signals of equal intensity. Since rotation about the C−Ph bond is rapid, the CH_2 protons will remain equivalent. (b) If the C−Ph bond is aligned off a mirror plane to make the CH_2 protons inequivalent, then four methyl signals of equal intensity should be observed (Scheme 2b). If the benzyl group preferentially lies over one of the dioxime wings and not over O−H···O, two out of four isomers will be absent and the remaining two isomers are superimposable. Therefore, only two sets of dmgH signals should be observed.

Scheme 2. Possibilities of Rotamers[a]

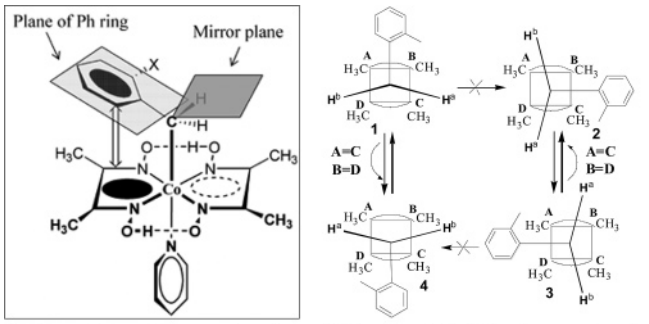

(a) Plane of phenyl ring and the mirror plane through CH_2. (b) (**A** = **C** and **B** = **D**) only when there is free rotation about the Co–C bond.

[a] The arc shows the O−H···O bridging. Four isomers are possible due to the rapid rotation of the Co−C bond provided CH_2 is diastereotropic due to the restriction in the C−Ph bond rotation. Since 1, 4 and 2, 3 are equivalent, two groups of diastereomers are formed. Each diastereomer will give two signals of dmgH(Me) since A = C and B = D. When the Co−C bond rotation is restricted, we can neglect the isomers 1 and 4 because the orientation of the benzyl is on O−H···O. The remaining two isomers may lead to 1:1 dmgH signals.

(2) *Rotation about the Co−C bond is fast, while rotation about the C−Ph bond is slowed.* For a phenyl substituted in the 2- or 3-position, slow rotation about the C−Ph bond results in the CH_2 protons being inequivalent provided that the plane of the phenyl ring is not aligned with the mirror plane running through the CH_2 group. In the structure in Scheme 2a, the phenyl group is at right angles to the plane. The result is that the C−Ph bond induces chirality through atropisomerism. The chirality will do exactly the same as the presence of a chiral atom in Me(CN)CHCo(dmgH)$_2$Py and MeCo(dmgH)$_2$NH(Me)CH_2Ph. No barrier to rotation about the Co−C bond is required, but rotamer preference is. The rotamers give inequivalent CH_2 protons and two dmgH methyl signals (Scheme 2). However, for this to happen, CH_2 must split before dmgH in order to induce atropisomerism, thus making dmgH inequivalent.

(3) *Rotation about both the Co−C and the C−Ph bond are slowed.* The presence of 2- or 3-substitution on the phenyl ring removes all the symmetry from the molecule. The CH_2 protons are inequivalent and the four methyl groups also become inequivalent. Thus four nonsuperimposable isomers will give four sets of dmgH signals. But in view of the π-interaction as stated in (1), two isomers will not be seen. Hence, only two isomers are possible and will produce two sets of signals.

Let us consider the low-temperature ^{1}H NMR spectra of dmgH complexes **2a**, **4a**, **8a**, **9a**, **10a**, and **11a**.

Dioxime. The chemical shift for the dioxime protons follows the order Br < H < Me. T_c also follows the same order. Compound **9a** with 2-Me as the substituent has a high ring current effect of the phenyl ring and has a high T_c, whereas

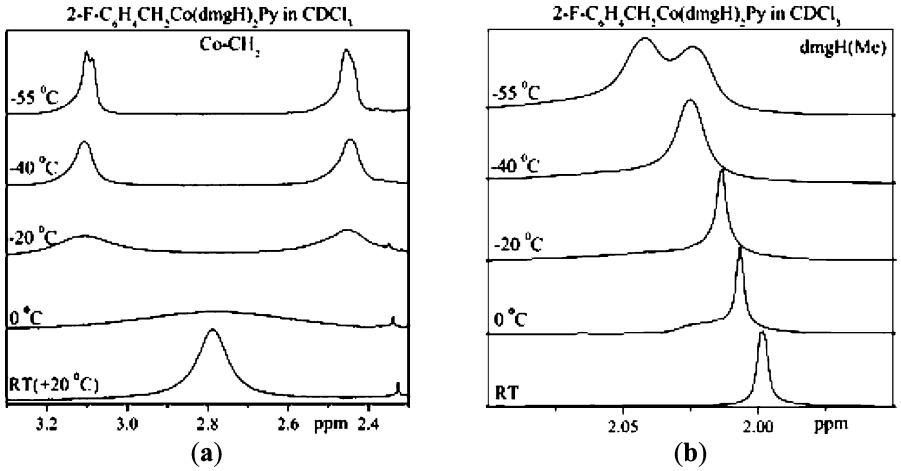

Figure 1. Variable-temperature ^{1}H NMR of CH_2-Co and dmgH(Me) signals for 2-F-$C_6H_4CH_2Co(dmgH)_2Py$ (**2a**).

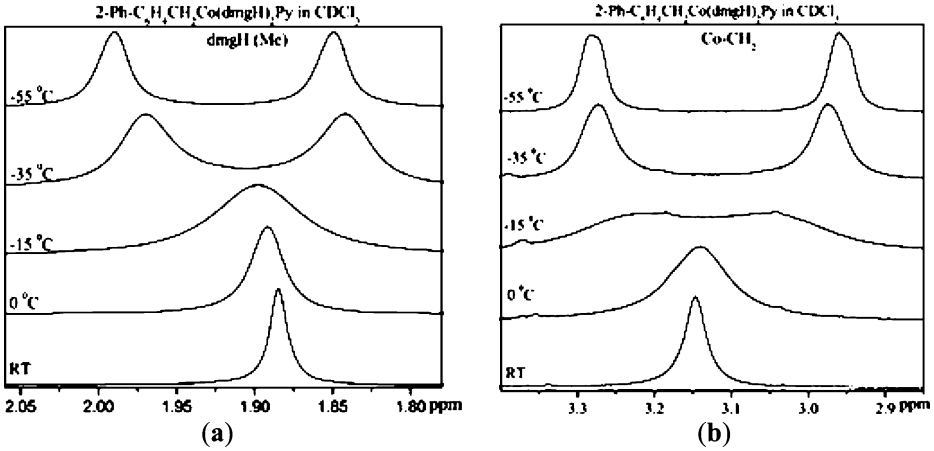

Figure 2. Variable-temperature ^{1}H NMR spectra of CH_2-Co and dmgH(CH_3) signals for 2-Ph-$C_6H_4CH_2Co(dmgH)_2Py$ (**8a**).

2-Br (**4a**) has a low δ value because of the lower ring current effect and has a low T_c. This implies that the nonequivalence of dioxime protons depends upon the electronic effect of the substituent and follows the same order as that of chemical shift. The results in 2-F (**2a**) (Figure 1) and 2-OMe (**10a**) (Figure S4, Supporting Information) support the same view. Although T_c for **4a** and **2a** is the same, $\Delta\delta$ (at −60 °C) between the two peaks is different; $\Delta\delta$ reflects the extent of π-interaction. So, the higher the electron density in the phenyl ring, the stronger the interaction between the axial and equatorial ligand and higher the T_c (i.e., coalescence occurs at higher temperature).

CH_2. The nonequivalence of CH_2 protons is not observed at room temperature, and it is rather difficult to understand on the basis of chemical shift order. The low-temperature NMR reveals much more useful information.

T_c of CH_2 protons in 2-Br (**4a**) is higher than in 2-Me (**9a**). This is opposite to the dioxime case. 2-F (**2a**) follows the same trend, whereas 2-OMe (**10a**) does not. Here, T_c for **10a** is higher (+2 °C) than expected and even higher than the dmgH protons (−20 °C) (Figure S4, Supporting information). This is quite surprising! This may be due to the steric factor and/or due to direct interaction of the OMe group with one of the CH_2 protons [the same was observed in xylylene-bridged dicobaloximes[12]]. The overall data suggest that the electron-withdrawing groups lead to higher T_c, and a direct interaction of the 2-substituent with the CH_2 protons is a possibility. The room-temperature NMR on these complexes also gave similar information.

The low-temperature study on the 2-Ph (**8a**) complex is particularly important since the interaction of CH_2 will depend upon the orientation of the phenyl group. The room-temperature NMR shows a singlet for CH_2 as well as dmgH(Me) due to the free rotation of the 2-Ph group.[19] However, these become nonequivalent at subzero temperature, and T_c for CH_2 and dmgH(Me) are −15 and −25 °C (Figure 2). The values indicate that the phenyl group is behaving like an electron-withdrawing group. It is, however, difficult to predict whether this nonequivalence is due to atropisomerism or due to the restricted rotation of the Co−C bond and/or C−Ph bond rotation.

To summarize, the nonequivalence of dmgH(Me) depends upon the Co−C bond rotation restriction. This in turn depends on the extent of interaction between the axial and equatorial ligand, and T_c depends upon the electronic effect of the substituent and follows the same order as that of chemical shift. In contrast, the nonequivalence of CH_2 shows the reverse order of electronic effect of the substituent and may also depend on its direct interaction with the 2-substituent.

Correlations. The effect of *ortho* substituent in ^{1}H NMR spectroscopy is well known,[20] and it is, in general, considered an electronic effect and is independent of the steric effect.[21] As the Taft *ortho* substituent constant (σ_o) increases, a decrease in the chemical shift of the observed hydrogen occurs.[21,22] We saw

(19) Interestingly, CH_2 appears as a doublet of doublets [2.66 (6.8 Hz) and 3.04 (7.2 Hz)] and dmgH appears as two singlets (1.87 and 1.92 ppm) in [2-Me-biphenyl-2′-$CH_2Co(dmgH)_2Py$] complex at room temperature due to atropisomerism.[11]

(20) Charton, M. *Prog. Phys. Org. Chem.* **1971**, *8*, 235.

(21) Tribble, M. T.; Traynham, J. G. In *Advances in Linear Free Energy Relationships*; Chapman N. B., Ed.; Plenum Press: New York, 1972; Chapter 4.

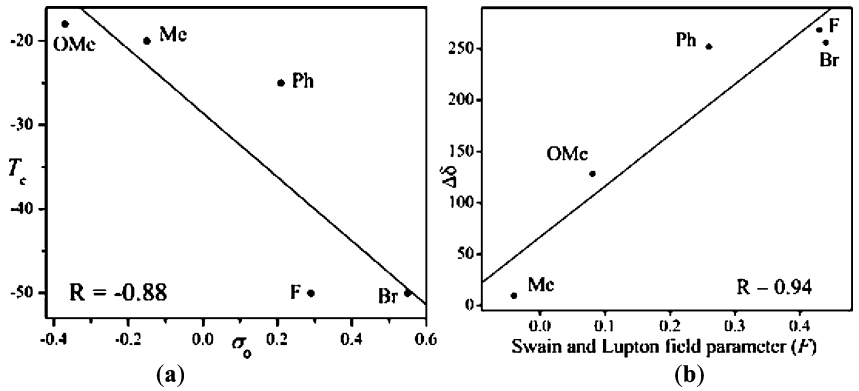

Figure 3. (a) Plot of T_c of dmgH(Me) signal against σ_o and (b) $\Delta\delta$ of Co−CH_2 signal against Swain and Lupton field parameter (F) for **2a**, **4a**, **8a**, **9a**, and **10a**.

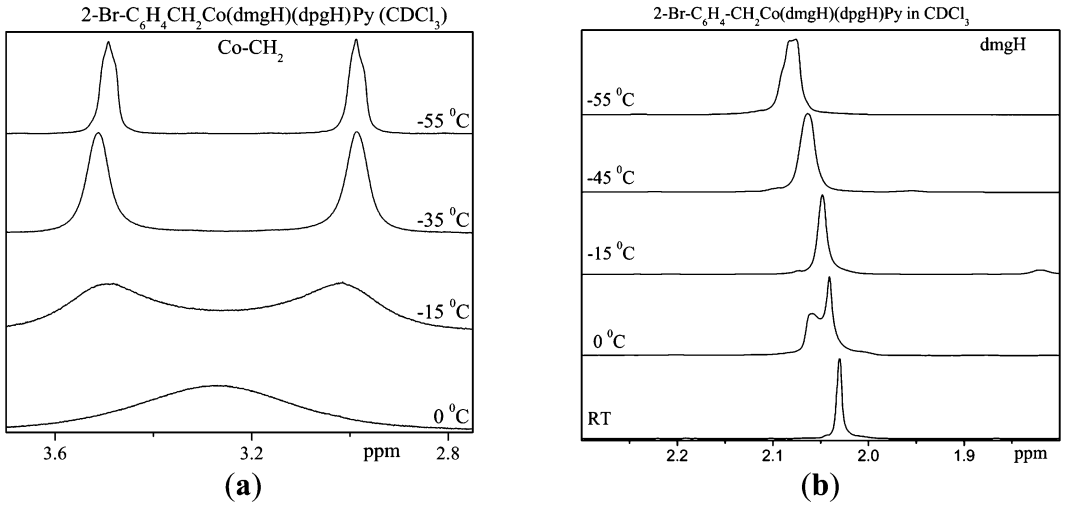

Figure 4. Variable-temperature ^{1}H NMR spectra of (a) CH_2−Co and (b) dmgH(Me) signals for 2-Br-C_6H_4-CH_2Co(dmgH)(dpgH)Py.

a good correlation with σ_o in *meta*-xylylene-bridged dicobaloximes.[12] Here we have observed no correlation between T_c or $\Delta\delta$ and σ_o for CH_2 protons (R = 0.06 and 0.33, respectively); however, dioxime protons correlate better with σ_o. For example, R is −0.88 and −0.80 for T_c and $\Delta\delta$, respectively, in **2**, **4**, **8**, **9**, and **10** (Figure 3). This suggests that with an increase in σ_o both T_c and $\Delta\delta$ decrease, and the dioxime(Me) protons are influenced predominantly by electronic factors, whereas the CH_2 protons are affected both by electronic and by some other factor. Among all the substituents 2-Ph deviates significantly in the correlations of the dioxime proton and R is rather poor. However the linear regression (R) becomes 0.96 if we exclude 2-Ph. This indicates that some factor besides electronic is also operating. The $\Delta\delta$ for CH_2 protons correlates better with the Swain and Lupton field parameter (F) (R = 0.94) (Figures 3), and T_c correlates with Taft's steric parameter (E_s) (R = 0.82).

The variable-temperature ^{1}H NMR study in 2,5-dimethyl complex (2,5-$Me_2C_6H_3CH_2$Co(dmgH)$_2$Py)[23] is interesting. T_c for CH_2 and dmgH(Me) is −20 and −12 °C, respectively. These are much lower, as expected, than for the 2-Me (**9a**) complex and are in accordance with the earlier discussion. The higher electron density in the benzyl group results in a lower T_c and thus supports the greater interaction with the dioxime. The same information was also obtained in room-temperature NMR: the dmgH(Me) is upfield shifted (1.94 ppm) compared to **1a** or **9a**. The presence of two methyl groups at the 2- and 5-positions further restricts the flipping of the C−Ph bond, thus lowering T_c of the CH_2 protons.

A ^{1}H NMR study of 2-Br-$C_6H_4CH_2$Co(dmgH)(dpgH)Py is even more interesting. The dmgH(Me) is a singlet even at −55 °C, but CH_2 starts splitting at −12 °C (Figure 4). The presence of a singlet seems surprising! The case study falls into category (3), where both C−Ph and Co−C bonds are restricted. At a temperature below −12 °C the C−Ph bond is restricted, and the atropisomerism induced due to inequivalent CH_2 should result in four nonequivalent isomers; thus four sets of dmgH (1:1:1:1) peaks should appear. The appearance of a singlet means that only one isomer is present, and this is possible only if the Co−C bond is partially or fully restricted (Scheme 3). The spectra in Figure 4b show the possibility of another isomer at around 0 °C. Can this be the isomer where the benzyl group is over dmgH rather than on the dpgH wing? Is it the intermediate temperature where the Co−C bond is partially restricted? Surprisingly, the O−H···O resonance also splits into two lines as the temperature is lowered. This is quite unique since it has never been observed before in any complex (Figure S5, Supporting Information).

Interestingly, the nonequivalence of dmgH and CH_2 is not observed in $PhCH_2SO_2$Co(dmgH)$_2$Py even at −55 °C. The X-ray structure shows that the benzyl group is oriented

(22) Hansch, C.; Leo, A.; Taft, R. W. *Chem. Rev.* **1991**, *91*, 165−195.

(23) ^{1}H NMR (400 MHz, $CDCl_3$): δ O−*H*···O: 18.35; Py: α-*H* 8.54 (d, 2H, J = 5.20 Hz), γ-*H* 7.65 (t, 1H, J = 7.41 Hz), β-*H* 7.26 (t, 2H, J = 6.44 Hz); benzyl: 6.84 (d, J = 7.59 Hz), 6.76 (d, J = 7.59 Hz), 6.62 (s, 1H); Co−C*H*$_2$: 2.89 (s, 2H); 2,5-C*H*$_3$: 2.23 (s, 3H), 2.04 (s, 3H); dmgH(C*H*$_3$) 1.94 (s, 12H).

(24) Ashcroft, M. R.; Bougeard, P.; Bury, A.; Cooksey, C. J.; Johnson, M. D. *J. Organomet. Chem.* **1985**, *289*, 403.

Scheme 3. 2-Br-C_6H_4-CH_2Co(dmgH)(dpgH)Py[a]

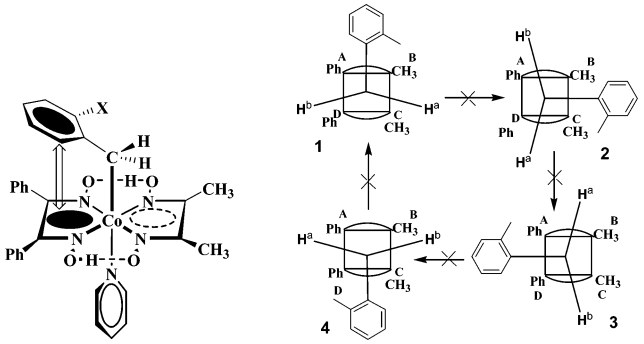

[a]A rapid rotation of the Co−C bond will form 4 isomers, of which none are superimposable. Thus dmgH(Me) will give 4 sets of signals (1:1:1:1). If the Co−C bond is partially or fully restricted, then we can neglect the orientations 1 and 4 (over O−H···O). Of the remaining two isomers only 3 will exist at the freezing temperature as per the crystal structure, where the benzyl group lies over the dpgH wing. Surprisingly, Figure 4b shows the possibility of another isomer at around 0 °C.

perpendicular to the dioxime plane and is too far away to have any interaction with the dioxime or CH_2.[25]

All the ^{1}H NMR chemical shifts have been interpreted on the basis of "through-space" interaction between the axial and equatorial ligand. ^{13}C NMR spectra give more conclusive evidence. Since ^{13}C works through bond and not through space, it is expected that ^{13}C chemical shifts for the dioxime group should not change much with the change in the substituent X in the benzyl group, as these are more than five bonds away from the axial group. This is what is observed also. ^{13}C NMR chemical shifts of the dioxime group are almost the same in all the complexes.

Conclusive evidence of the π-interaction with the dioxime ring current is seen in pyrazine-bridged dicobaloximes; for example, the pyrazine-bridged alkyl complex attains the staggered conformation, whereas the benzyl analogue acquires the eclipsed conformation.[26] The same types of π-interaction between the axial and equatorial ligand have been reported by Randaccio et al.[27] in $RCo(DBPh_2)_2B$ and Styne et al.[28] in $LFe^{II}(DBPh_2)_2L'$, where this interaction defines the ligand's orientation.

The weak interactions between the axial and equatorial ligands cause restriction of Co−C and/or C−Ph bond rotation and seem to be responsible for the nonequivalence of dmgH methyl and CH_2 protons. It also points to the possibility that such weak interactions (adenine to side chain methyl in the case of AdoCbl) might cause the stabilization of adenine during the Co−C bond rupture and thus differentiates it from MeCbl. If the weak π-interaction is important, as the preliminary results show, the nonequivalence of the dmgH or CH_2 groups will occur irrespective of the nature of dioxime, and the extent of nonequivalence will depend on the ring current and puckering in the dioxime. To see the generality of this behavior, we have carried out the low-temperature study of the gH complex (**4c**).

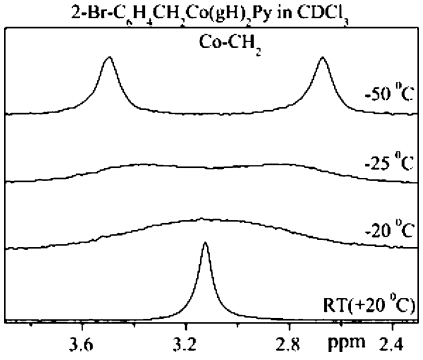

Figure 5. Variable-temperature ^{1}H NMR spectra of CH_2−Co signal for 2-Br-$C_6H_4CH_2Co(gH)_2Py$ (**4c**).

The CH_2 protons split at much lower temperature (−23 °C), as expected, than the corresponding T_c in the dmgH complex (**4a**) (Figure 5). Also, we could not achieve T_c for the gH protons even at −60 °C. This is not surprising since we anticipated it to be much lower than the corresponding T_c (−50 °C) in the dmgH complex (**4a**). This suggests weaker interaction between axial and equatorial dioxime in **4c**. The weaker interaction is due to the lower bulkiness of the dioxime moiety and lower electron density in the $Co(dioxime)_2$. The observation is as per our expectation and fits well with the interpretation given above. A similar observation was made earlier in the 2-substituted *meta*-xylylene-bridged dicobaloxime systems.[12]

X-ray Crystal Structure. Orange crystals were obtained by slow evaporation of solvent from the solution of complexes **9a**, **11a**, **1b**, and **4c** (CH_2Cl_2/ MeOH/hexane) in the refrigerator. The "diamond" diagrams of molecular structures along with selected numbering scheme are shown in Figures 6 and 7. Selected bond lengths, bond angles, and structural parameters are given in Table 3 and are compared with those of the related cobaloximes. The geometry around the central cobalt atom is distorted octahedral with four nitrogen atoms of the dioxime in the equatorial plane and pyridine and benzyl axially coordinated.

The structural studies on cobaloximes have focused mainly on four points: (a) the axial Co−N and the Co−C bond length, (b) the puckering of the equatorial dioxime ligand, i.e., butterfly bending angle (α), (c) the torsion angle between the axial base pyridine and equatorial ligand, and the deviation of the cobalt atom from the mean equatorial N_4 plane (*d*). These points assist in defining the *cis* or *trans* influence of axial as well as equatorial ligands.

The Co−C [2.048(7), 2.055(4), 2.056(5), 2.061(4) Å] and Co−N5 bond distances [2.060(7), 2.047(5), 2.061(4), 2.054(3) Å] in **9a**, **11a**, **1b**, and **4c** do not differ significantly, and also they are similar to the reported values in the corresponding $BnCo(dmgH)_2Py$ cobaloximes.[13a]

The cobalt atom deviates from the mean equatorial N_4 plane, and the deviations (*d*) are −0.0275, −0.0208, +0.0209, and +0.0225 Å. The deviation is small and is toward the axial organic group in **1b** and **9a** and toward pyridine in **4c** and **11a**.

In general, α and *d* respond essentially to the difference in steric bulk between the two axial ligands.[1b] We will restrict our discussion to the changes in the axial organic group since the axial base ligand, pyridine, is same in all the complexes in our study. An increase in the bulk in R increases α; for example, the values are 5.8° and −5.2° for R = Et and CH_2CMe_3.[1b] In an extreme case a change of Me to adamantyl in $RCo(dmgH)_2Py$ changes α from +1.86° to −10.6°.[1b]

(25) Chadha, P.; Gupta, B. D.; Mahata, K. *Organometallics* **2006**, *25*, 92.

(26) Mandal, D.; Gupta, B. D. *J. Organomet. Chem.* **2005**, *690*, 3746.

(27) (a) Dreos, R.; Tauzher, G.; Vuano, S.; Asaro, F.; Pellizer, G.; Nardin, G.; Randaccio, L.; Geremia, S. *J. Organomet. Chem.* **1995**, *505*, 135. (b) Asaro, F.; Dreos, R.; Geremia, S.; Nardin, G.; Pellizer, G.; Randaccio, L.; Tauzher, G.; Vuano, S. *J. Organomet. Chem.* **1997**, *548*, 211. (c) Dreos, R.; Geremia, S.; Nardin, G.; Randaccio, L.; Tauzher, G.; Vuano, S. *Inorg. Chim. Acta* **1998**, *272*, 74.

(28) (a) Stynes, D. V.; Leznof, D. B.; de Silva, D. G. A. H. *Inorg. Chem.* **1993**, *32*, 3989. (b) Stynes, D. V. *Inorg. Chem.* **1994**, *33*, 5022. (c) Vernik, I.; Stynes, D. V. *Inorg. Chem.* **1996**, *35*, 6210, and references therein.

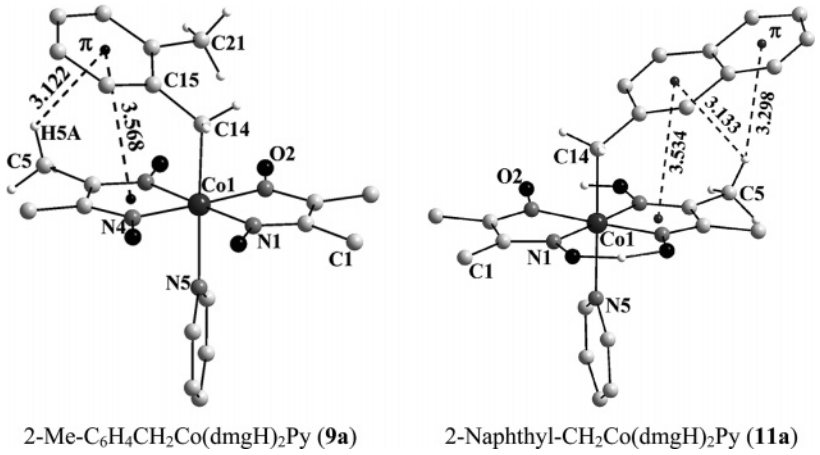

2-Me-$C_6H_4CH_2Co(dmgH)_2Py$ (**9a**) 2-Naphthyl-$CH_2Co(dmgH)_2Py$ (**11a**)

Figure 6. Molecular structure of **9a** and **11a**.

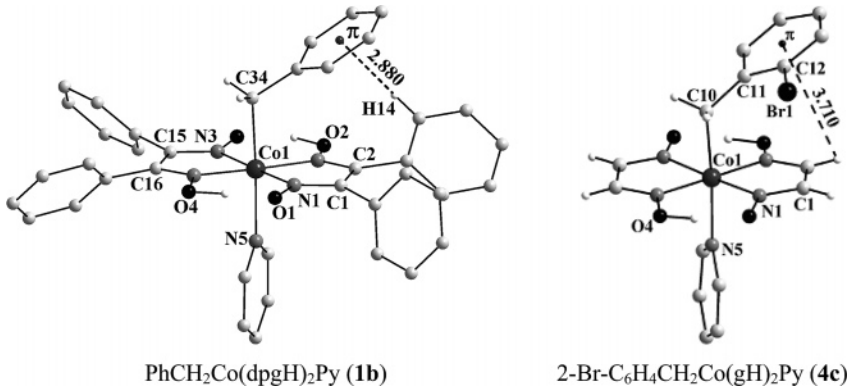

$PhCH_2Co(dpgH)_2Py$ (**1b**) 2-Br-$C_6H_4CH_2Co(gH)_2Py$ (**4c**)

Figure 7. Molecular structure of **1b** and **4c**.

Table 3. Crystal Data, Selected Bond Lengths (Å), Bond Angles (deg), and Torsion Angles (deg) in 9a, 11a, 1b, 4c, and 1a[12a]

param	9a	11a	1b	4c	1a[12a]
Co−C_{ax}	2.048(7)	2.055(4)	2.056(5)	2.061(4)	2.064(15)
Co−N_{ax}	2.060(7)	2.047(5)	2.061(4)	2.054(3)	2.056(14)
C−Ph[a]	1.491(8)	1.485(5)	1.477(8)	1.483(6)	1.474
N5−Co−C_{ax}	176.1(3)	177.7(2)	176.8(2)	175.57(13)	177.1(1)
Co−C−C	118.1(4)	115.2(4)	117.9(3)	115.5(3)	116. 6 (3)
N5−Co−C−C	−142.7	140.3	155.1	−178.2	158.8
N_{eq}−Co−C−C[b]	−61.1	−17.0	−12.7	−3.1	−20.1
Co−C−C−C[c]	−90.9	−91.2	−91.65	−101.46	−93.94
d (Å)	−0.0208	+0.0225	−0.0275	+0.0209	−0.0371
α (deg)	1.74	6.90	1.75	2.68	1.86
τ (deg)	88.96	88.75	88.96	74.36	
π···*π* (Å)	3.568(10)	3.534	3.748(3)	3.717	3.564(19)
C−H···*π* (Å)	3.122(9)	3.133 (3.298)	2.880(4), 3.189	3.710	3.183(22)

[a] (C−Ph) =1.488 Å [2-NO_2-C_6H_3-[$CH_2Co(dmgH)_2Py]_2$].[11] [b] Torsion angle defines the Co−C bond orientation; N_1−Co−C−C = +62.34° in 2-vinyl-$C_6H_4CH_2Co(dmgH)_2Py$[10] and the order is **4c** < **1b** < **11a** < **1a** < **9a** < 2-vinyl. [c] Co−C−C−C torsion angle defines the C−Ph bond rotation (2-X-C_6H_4 orientation); torsion angle is −101.3° in 2-NO_2-C_6H_3-[$CH_2Co(dmgH)_2Py]_2$.

In the present systems α is positive in all cases, and any change in this value will be a measure of interaction of the axial with the equatorial ligand. A high α value (6.90°) in **11a** indicates greater interaction of 2-naphthyl than the substituted benzyl group. The value remains almost the same in benzyl (**1a**) and 2-Me (**9a**). This indicates that Me at the 2-position does not interact with the dioxime. This is justified since the 2-Me group is oriented away from the dioxime. However, α is greater in **4c** than **1a** and **9a** since the steric bulk of the dioxime decreases as we move from dmgH to gH. The higher value can also be due to an additional interaction of Br with the dioximes ring current.

The ^{1}H NMR data were effectively rationalized on the basis of the orientation of the benzyl group and its interaction with the dioxime or CH_2 group. It is now certain that the nonequivalence of dioxime protons is due to the hindered rotation of the Co−C bond, which depends solely on the interaction between the axial benzyl and equatorial dioxime. The orientation of the benzyl group becomes, therefore, the key factor. The question is how precisely can we ascertain the effect of orientation from the X-ray study?

This can be ascertained from the magnitude of interaction between the axial and equatorial moiety. The *π*-interaction is more intense in dmgH or dpgH complexes than in gH complexes. The C−H···*π* distances are almost the same in dmgH complexes, **1a**, **9a**, and **11a** (3.185(2), 3.122(9), and 3.133(3) (3.298(3)) Å, respectively), whereas it is significantly shorter in the dpgH complex **1b** (2.880(4) Å) and longer in **4c** (3.710(2) Å). The C−H···*π* interaction in the dioximes follows the order dpgH > dmgH > gH. T_c and $\Delta\delta$ for dioxime protons also follow

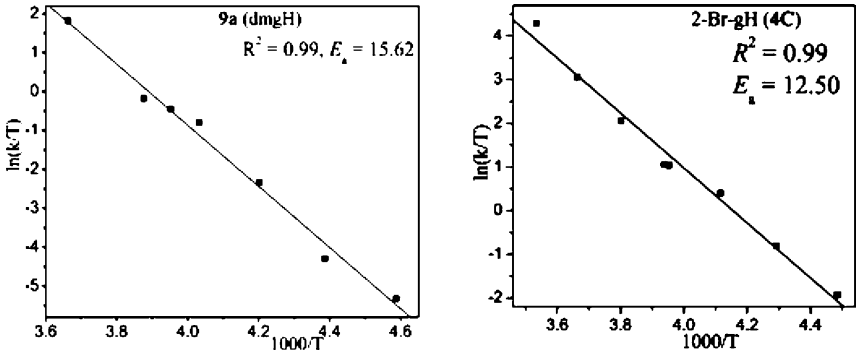

Figure 8. Plot of ln(k/T) and 1000/T (K) for dmgH(Me) in **9a** and Co−CH_2 in **4c**.

Table 4. Activation Energy (E_a) (kcal/mol)[a]

	F (**2a**)	Br (**4a**)	Ph (**8a**)	CH_3 (**9a**)	OMe (**10a**)	Naph (**11a**)	Br (gH) (**4c**)
Co−CH_2 Nonequivalence (C−Ph Bond Rotation)							
T_c (°C)	−7	−14	−15	−45	+2	−30	−23
E_a	10.26	10.52	15.71		11.09	11.71	12.50
dmgH(Me) Nonequivalence (Co−C Bond Rotation)							
T_c (°C)	−50	−50	−25	−20	−20	−23	
E_a			17.07	15.62	8.79	11.94	

[a] The calculated error is ±0.25 using 3 K temperature approximation.

the same order dmgH > gH in the present study. Similar information was obtained in the 2-substituted *meta*-xylylene-bridged dicobalt systems (dpgH > dmgH > gH).[11,12]

The $^2J_{HH}$ of ca. 6 Hz suggests restriction of C−Ph bond rotation, thus making CH_2 diastereotopic. This may arise if there is some double-bond character in the C−Ph bond and the hybridization of the CH_2 carbon is intermediate between sp^2 and sp^3. However the X-ray data show the C−Ph bond distance to be identical to toluene (∼1.485 Å).

We have considered some more structural parameters in order to distinguish between the restriction of Co−C and C−Ph bond rotation.

The torsion angle N_{eq}−Co−C−C [Figures 6, 7 and Table 3] defines the position (orientation) of the benzyl group over the Co(dioxime)$_2$ moiety. The negative value [**1a**, −20°; **1b** (N2−Co1−C34−C35), −12°] shows that the C−Ph bond lies over the dioxime ring current (negative value means clockwise rotation of the C−Ph bond with respect to the Co−N_{eq} bond and vice versa). A significantly high value, (N4−Co1−C14−C15) −61.1°, in **9a** shows the phenyl ring to be over dioxime and the 2-Me group is more over O−H···O. On the other extreme, a very low value, (N2−Co1−C10−C11) −3.14°, in **4c** indicates that the C−Ph bond lies over the C═N bond and Br over the dioxime ring current, and Br also has additional interaction with the dioxime along with the phenyl ring (a similar observation was made by Steinborn et al.[10] in 2-F-cyclohexyl cobaloximes). This may have caused the higher α value in 2-Br (**4c**) as compared to 2-Me (**9a**).

We have yet to confirm if it is a general phenomenon that the electron-releasing groups in the phenyl ring give a high torsion angle and the electron-withdrawing groups give a low or zero torsion angle. A high torsion angle (+62.34°) in the reported 2-vinyl-$C_6H_4CH_2$Co(dmgH)$_2$Py[11] can result only if there is no interaction of the vinyl group with the dioxime ring current.

Activation Energy Calculations

The above discussion has shown that the weak interactions between the axial and equatorial ligand cause restriction of the Co−C and/or C−Ph bond rotation and seem to be responsible for the nonequivalence of dmgH(Me) and CH_2 protons. The dominance of one process over the other depends upon the substituent present at the 2-position and the activation energy associated with these processes. It is important if one is able to calculate the E_a for the rotation of the Co−C and C−Ph bond.

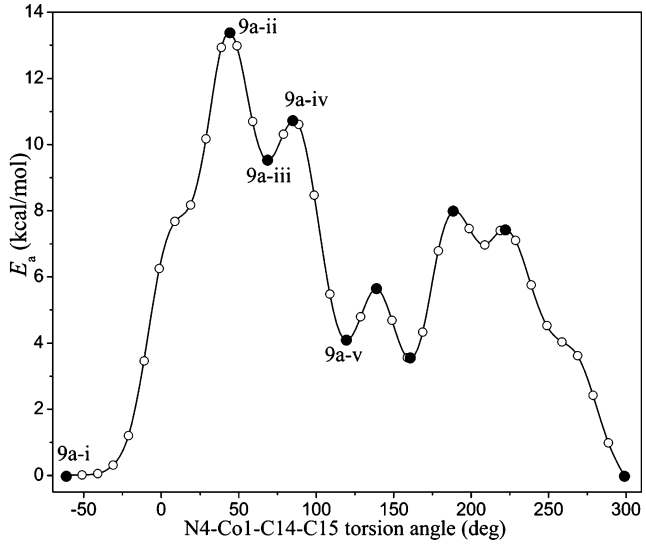

Figure 9. Conformational energy diagram for Co−C bond rotation in 2-Me-$C_6H_4CH_2$Co(dmgH)$_2$Py (**9a**). Equilibrium structure and transition states are marked by solid circles. Structures **9a**-(**i** to **iv**) are shown in Figure 10, where the reference atoms for the torsion angle N4−Co1−C14−C15 are given.

Evaluation of Rate Constants. As the temperature is varied from that where the rate of exchange is low through values of intermediate exchange rates to rapid exchange, a series of approximations is available for the calculation of lifetimes according to the procedure proposed by Gasparro.[29] Although these approximate methods provide somewhat less accurate results, they show a meaningful treatment of the data obtained by an NMR study of a chemical rate process.

(29) Gasparro, F. P.; Kolodny, N. H. *J. Chem. Educ.* **1977**, *54*, 258.

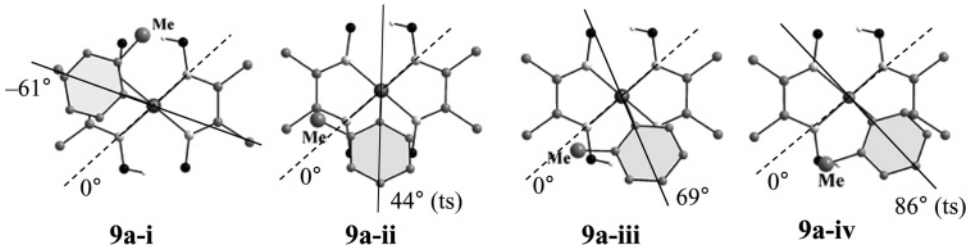

Figure 10. Calculated structures of rotational conformers of **9a** due to Co−C bond rotation (**9a-i**, **iii**, equilibrium structures, N4−Co1−C14−C15 = −61/+68.8°; **9a-ii**, **iv**, transition states, N4−Co1−C14−C15 = +43.9/+85.8°) (view from above, pyridine ligand is omitted).

The data are divided into three groups corresponding to slow change and intermediate exchange, coalescence temperature, and fast exchange. The rates (k) are calculated from the equations for these three types of exchange processes (shown below).

$$k_c = \frac{\pi\Delta\nu_o}{\sqrt{2}}$$

for coalescence temperature (T_c) (1)

$$k = \pi[(W)_{1/2} - (W_o)_{1/2}]$$

for very slow exchange rate (2)

$$k = \pi\left[\frac{\Delta\nu_o^{\,2} - \Delta\nu_e^{\,2}}{2}\right]^{1/2}$$

for intermediate exchange rate close to T_c (3)

$$k = \frac{\pi\Delta\nu_o^{\,2}}{2}[(W)_{1/2} - (W_o)_{1/2}]^{-1}$$

for exchange rate faster than T_c (4)

where ν_o = highest separation between two peaks (at the slowest exchange); ν = separation between two peaks at the given temperature; $(W_o)_{1/2}$ = line width at the half of the peak maxima (at the slowest exchange); and $W_{1/2}$ = line width at the half of the peak maxima at the given temperature.

Equations 1−4 are used to calculate k (Table S3, Supporting Information). Figure 8 shows the plot of ln(k/T) versus 1000/T (K); the slope of this plot gives the value for the activation energy. Using the values of k extending over the entire temperature range, E_a for **10a** is found to be 11.09 kcal/mol for CH_2 protons and 8.79 kcal/mol for dmgH(Me) protons. In some cases the lowest temperature could not be achieved, and hence their E_a could not be calculated.

A summary of the free energies of activation for representative complexes as calculated by line shape analysis of the variable-temperature ^{1}H NMR data using the Eyring equation is presented in Table 4. Direct comparisons of free energies of activation are only proper if the data are collected at similar temperatures. Since each complex in Table 4 has a different coalescence temperature, exact comparisons cannot be made. The higher the activation energy, the higher the barrier for rotation, and in the same compound E_a follows T_c for Co−C and C−Ph bond rotation. However, the comparison is difficult between cobaloximes with different substituents or different dioximes.

Theoretical Calculations

To get further insight into the hindered rotation, quantum chemical calculations on the DFT level of theory have been performed. As a case study, we have selected 2-Me (dmgH) (**9a**) and 2-Br (gH) (**4c**) complexes. Closed-shell single-point calculations in **9a** and **4c** were performed using the atomic coordinates provided by the X-ray structures of these compounds.

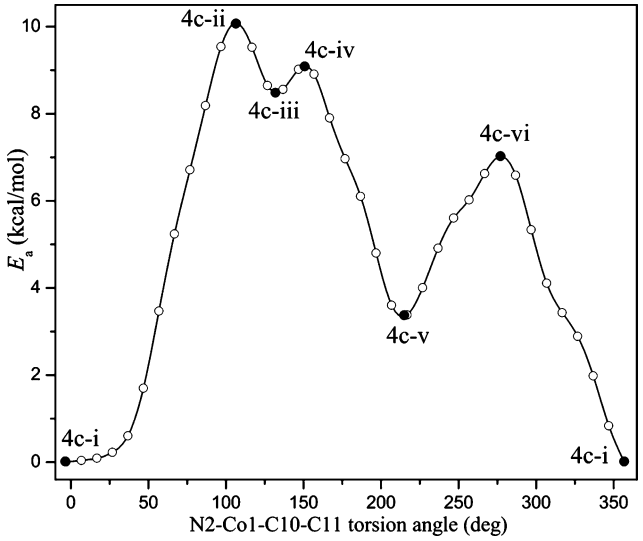

Figure 11. Conformational energy diagram for Co−C bond rotation in 2-Br-$C_6H_4CH_2$Co(gH)$_2$Py (**4c**). Equilibrium structure and transition states are marked by solid circles. Structures **4c**-(**i** to **vi**) are shown in Figure 12, where the reference atoms for the torsion angle N2−Co1−C10−C11 are given.

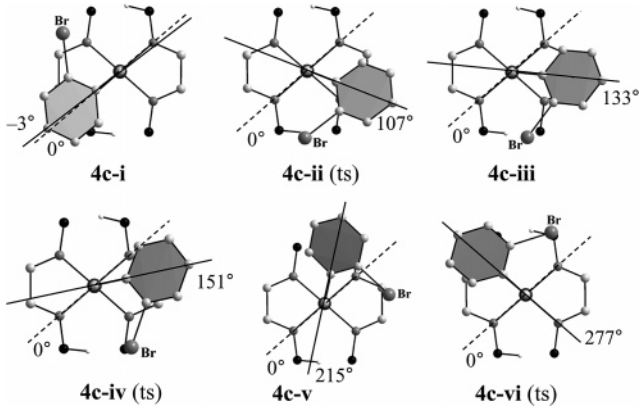

Figure 12. Calculated structures of rotational conformers of **4c** due to Co−C bond rotation (**4c-i**, **iii**, equilibrium structures, N2−Co1−C10−C11 = −3.1/+132.6°; **4c-ii**, **iv**, transition states, N2−Co1−C10−C11 = +107.2/+151.6°) (view from above, pyridine ligand is omitted).

The orientation of the axial 2-Me-$C_6H_4CH_2$ ligand with respect to the equatorial (dmgH)$_2$ ligand was measured by means of the torsion angle N4−Co1−C14−C15 (−61.05°), and the single-point calculations were performed at each point after rotation of the torsion angle by 10°. In doing so, the Co−C bond rotation is considered. The conformational energy diagram

Table 5. Energies of Equilibrium Structure (ES) and Transition State (TS) (ΔE in kcal/mol) for Co−C and C−Ph Bonds in 9a and 4c

	9a		4c	
		Co−C		
	N4−Co1−C14−C15	ΔE	N2−Co1−C10−C11	ΔE
ES (global min.)	−61.0° (**9a-i**)	0.0	−3.1° (**4c-i**)	0.0
TS (global max.)	44.0° (**9a-ii**)	13.4	107.0° (**4c-ii**)	10.7
ES (local min.)	68.8° (**9a-iii**)	9.5	132.9° (**4c-iii**)	9.1
TS (local max.)	85.8° (**9a-iv**)	10.7	150.9° (**4c-iv**)	9.7
		C−Ph		
	Co1−C14−C15−C16	ΔE	Co1−C10−C11−C12	ΔE
ES (global min.)	89.9° (**9a-I**)	0.0	−101.5° (**4c-I**)	0.0
exptl (NMR) TS			−133.5° (**4c-II**)	12.5
TS (global max.)	1.5° (**9a-II**)	151.0	−190.5° (**4c-III**)	110.0
ES (local min.)	−70.1° (**9a-III**)	1.7	−254.5° (**4c-IV**)	4.6

(Figure 9) shows that the rotation of the 2-Me-$C_6H_4CH_2$ ligand around the Co−C bond by a total of 180° (giving a complete picture due to the C_2 symmetry of the $(dmgH)_2$ ligand)[30] results in two minima (**9a-i** and **9a-iv**) and two maxima (**9a-iii** and **9a-v**) of potential energy. In **9a-i** the Ph ring is over the dioxime ring current (torsion angle N4−Co1−C14−C15 = −61.05°), and in **9a-iv** (N4−Co1−C14−C15 = 68.8°) it lies above one N−O bond (Figure 10). Similarly, the conformational energy diagram (Figure 11) shows the rotation of the 2-Br-$C_6H_4CH_2$ ligand around the Co−C bond by 10° (Figures 11 and 12). All the TS and ES energies and the corresponding torsion angles are given in Table 5.

In the (global) transition state (**9a-iii**) with the highest potential energy, the Ph ring lies above the O−H···O bridge, and in the local transition state (**9a-v**) it lies over the C═N bond (Figure 10). The energy barrier for the Co−C bond rotation in **9a** (ΔE = 13.4 kcal/mol, energy difference between **9a-i** and **9a-iii**) matches well with the experimental value (15.6 kcal/mol) of the E_a derived from the variable-temperature ^{1}H NMR, whereas it is 10.6 kcal/mol in **4c**. A high experimental value of 15.6 kcal/mol suggests that the solid state hindrance adds ∼2 kcal/mol to the gas phase rotational barrier.[31]

A conformational energy diagram for the rotation of 2-Br-$C_6H_4CH_2$ around the C−Ph bond by 180° in **4c** is shown in Figure 13. The C−Ph bond orientation is defined by the torsion angle Co1−C10−C11−C12 (−101.46°), and the single-point calculations were performed at each point after a rotation of the torsion angle by 10°. The energy barrier for the C−Ph bond rotation in **4c** matches well with the experimental value from NMR up to a rotation of −133.5° (**4c-II**). However, after this point, there is a steep increase in energy up to 90° rotation (**4c-III**). There are two minima, at −101.5° (**4c-I**) and −254.5° (**4c-IV**). The most stable conformation is **4c-I**, since it is 4.6 kcal/mol lower in energy than **4c-IV**. A further increase in the torsion angle causes a steep increase in energy (**4c-V**) due to the interaction of Br with the dioxime (Figure 14). The overall information from the ΔE for C−Ph bond rotation supports our earlier discussion on the NMR that the phenyl group only flips and does not undergo full rotation. The conformational energy diagram for C−Ph bond rotation in **9a** also gives the same information (Figures 15 and 16).

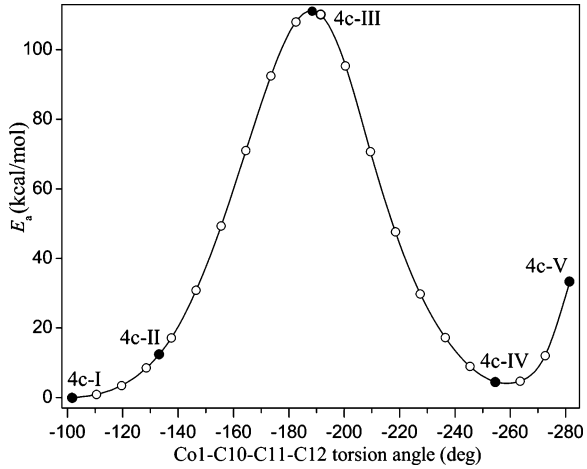

Figure 13. Conformational energy diagram for C−Ph bond rotation in **4c**. Equilibrium structure and transition state are marked by solid circles. **4c-II** is marked to indicate the activation energy (ΔE) is identical with the E_a calculated from the variable-temperature NMR.

Conclusions

The dioxime protons and the cobalt-bound CH_2 appear as a singlet at room temperature but show nonequivalence in the ^{1}H NMR at subzero temperature. The nonequivalence arises due to the restricted rotation of the Co−C and C−Ph bonds, and these two different processes may have the same/different origin. The weak interaction between the axial and equatorial ligand causes the restriction to the rotation of the Co−C and C−Ph bonds. The nature of the substituent at the 2-position as well the electron density in the dioxime affects the extent of nonequivalence. The C−Ph bond rotation is slow with electron-withdrawing groups, while the electron-donating groups slow the Co−C bond rotation. The activation energy calculation (E_a) from the variable-temperature ^{1}H NMR also shows the dependence of the Co−C and C−Ph bond rotation on both dioximes as well as the 2-substituents. This is also supported by the theoretical studies (DFT). Conformation energy diagrams derived from the theoretical calculations for C−Ph bond rotation indicate that the phenyl group only flips and does not undergo full rotation.

Experimental Section

$ClCo(dmgH)_2Py$,[32a] $ClCo(dpgH)_2Py$,[32b] and $ClCo(gH)_2Py$[33] were prepared according to the literature procedure. ^{1}H and ^{13}C spectra

(30) Since the atomic coordinates taken from the X-ray crystal structure are not C_2 symmetric, we have performed calculations up to 360°.

(31) Karlen, S. D.; Ortiz, R.; Chapman, O. L.; Garcia-Garibay, M. A. *J. Am. Chem. Soc.* **2005**, *127*, 6554.

(32) (a) Schrauzer, G. N. *Inorg. Synth.* **1968**, *11*, 61. (b) López, C.; Alvarez, S.; Font-Bardia, M.; Solans, X. *J. Organomet. Chem.* **1991**, *414*, 245.

(33) (a) Toscano, P. J.; Swider, T. F.; Marzilli, L. G.; Bresciani-Pahor, N.; Randaccio, L. *Inorg. Chem.* **1983**, *22*, 3416. (b) Gupta, B. D.; Yamuna, R.; Singh, V.; Tewari, U. *Orgnometallics* **2003**, *22*, 226.

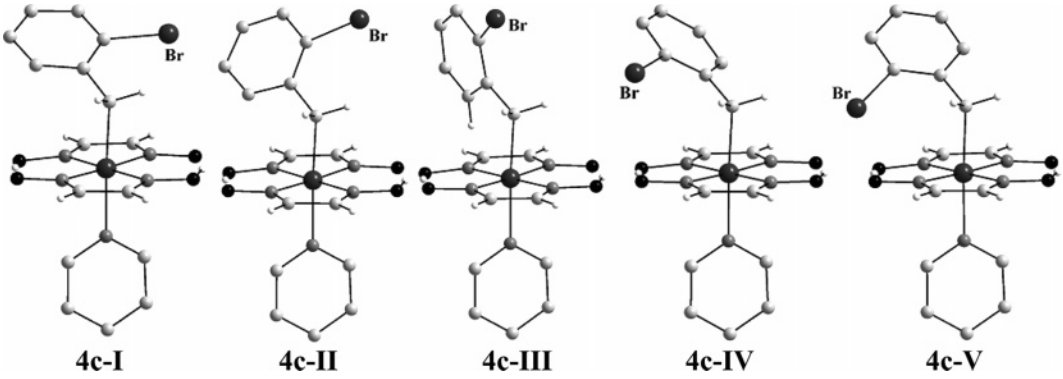

Figure 14. Calculated structures of rotational conformers of 2-Br-$C_6H_4CH_2Co(gH)_2Py$ (**4c**) due to C−Ph bond rotation (**4c-I**, **IV**, equilibrium structures, Co1−C10−C11−C = −101.5/−254.5°; **4c-III**, transition state, torsion angle = −190.5°). **4c-V** shows when Br directly interacts with dioxime and the sharp increase in ΔE.

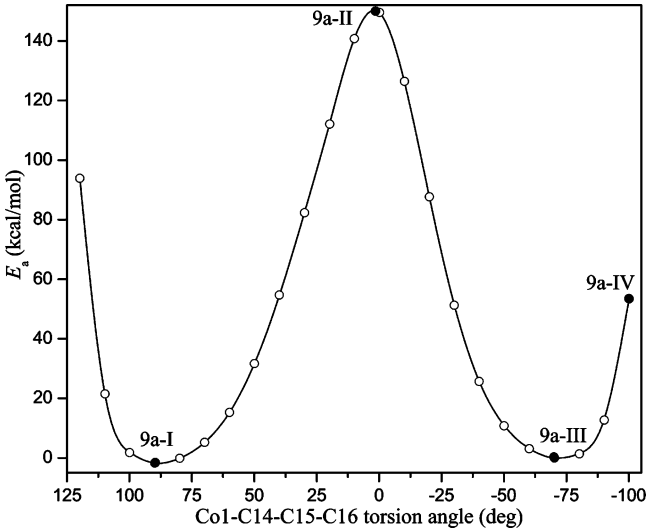

Figure 15. Conformational energy diagram for C−Ph bond rotation in **9a**. Equilibrium structure and transition state are marked by solid circles.

were recorded on a JEOL JNM LA 400 FT NMR spectrometer (400 MHz for ^1H and 100 MHz for ^{13}C) in $CDCl_3$ solution with TMS as internal standard. NMR data are reported in ppm. UV−visible spectra were recorded on a JASCO V-570 spectrophotometer in dichloromethane (dry) and methanol. Elemental analysis was carried out at the Regional Sophisticated Instrumentation Center, Lucknow. CHN analysis and yields are tabulated in Table S2 (Supporting Information). The variable-temperature ^1H NMR spectra were recorded on a JEOL JNM Lambda 400 FT NMR spectrometer (at 400 MHz) in $CDCl_3$, and CD_2Cl_2 was used as solvent for measurements below −60 °C.

The *ortho*-substituted benzyl halides were either purchased from Aldrich Chemical Co. or prepared by known literature procedures. $CoCl_2 \cdot 6H_2O$, dimethylglyoxime (Merck India), and glyoxime (Fluka) were used without further purification. Diphenylglyoxime (Lancaster) was washed with small portions of methanol before use.

X-ray Crystal Structure Determination and Refinements. Orange crystals were obtained by slow evaporation of the solvent (chloroform/methanol/*n*-hexane) for **9a**, **11a**, **1b**, and **4c**. Single-crystal X-ray data were collected using graphite-monochromated Mo Kα radiation (λ = 0.71073 Å) on a Bruker SMART APEX CCD diffractometer at 100 K for **11a**, **1b**, and **4c**, and the data were collected at 293 K on a CAD4 for **9a**. The linear absorption coefficients, scattering factors for the atoms, and the anomalous dispersion corrections were taken from International Tables for X-ray Crystallography.[34a] The data integration and reduction were processed with SAINT[35] software. An empirical absorption correction was applied to the collected reflections with SADABS[36] using XPREP.[37] All the structures were solved by the direct method using SIR-97[38] and were refined on F^2 by the full-matrix least-squares technique using the SHELXL-97[34b] program package. All non-hydrogen atoms were refined anisotropically in all the structures. The hydrogen atoms of the OH group of oxime were located on difference Fourier maps and were constrained to those difference Fourier map positions. The hydrogen atom positions or thermal parameters were not refined but were included in the structure factor calculations. The pertinent crystal data and refinement parameters are compiled in Table S4, Supporting Information.[39] CIF files for the subject compounds are deposited with the Cambridge Crystallograpic Data Centre (CCDC nos. **9a** 282006, **11a** 602782, **1b** 614785, **4c** 614784 contain the supplementary crystallographic data). Copies of the data can be obtained free of charge from the Director, CCDC, 12 Union Road, Cambridge CB2 1EX, UK (fax: +44-1223-336033; e-mail: deposit@ccdc.cam.ac.uk; or www: http://www.ccdc.cam.ac.uk/).

Computational Details. The density functional theory (DFT) calculations were performed with the Gaussian 03 suite of programs[40] using Becke's three-parameter hybrid exchange functional[41] and the Lee−Yang−Parr correlation functional (B3LYP).[42] The double-ζ basis set of Hay and Wadt (LanL2DZ) with an effective core potential (ECP) was used for Co to represent the innermost electrons of the cobalt atom,[43] and the main group elements were described using the 6-31G(d) basis sets. The calculations were performed in the gas phase, and the solvation effects were not considered. Closed-shell single-point calculations in **9a** and **4c** were performed using the atomic coordinates provided by the X-ray structures of these compounds.

(34) (a) *International Tables for X-ray Crystallography*; Kynoch Press: Birmingham, England, 1974; Vol. IV. (b) Sheldrick, G. M. *SHELXL-97: Program for Crystal Structure Refinement*; University of Göttingen; Göttingen, Germany, 1997.

(35) *SAINT+*, 6.02 ed.; Bruker AXS: Madison, WI, 1999.

(36) Sheldrick, G. M. *SADABS, Empirical Absorption Correction Program*; University of Göttingen: Göttingen, Germany, 1997.

(37) *XPREP*, 5.1 ed.; Siemens Industrial Automation Inc.: Madison, WI, 1995.

(38) Altomare, A.; Burla, M. C.; Camalli, M.; Cascarano, G. L.; Giacovazzo, C.; Guagliardi, A.; Moliterni, A. G. G.; Polidori, G.; Spagna, R. *J. Appl. Crystallogr.* **1999**, *32*, 115.

(39) Crystal data for $C_6H_5CH_2Co(dpgH)_2Py$: $C_{40}H_{34}CoN_5O_4$, M_r = 707.65, crystal size 0.35 × 0.25 × 0.20 mm; triclinic; space group $P\bar{1}$; a = 10.5320(13) Å, b = 11.9152(14) Å, c = 14.7834(17) Å; α = 97.161(2)°, β = 95.269(2)°, γ = 112.790(2)°; V = 1677.0(3) Å^3; Z = 2; ρ = 1.401 Mg m^{-3}; T = 100(2) K; reflections measured/unique 11 171/7963. Final R = 0.0789 (R_w = 0.1513). Crystal data for 2-Br-$C_6H_4CH_2Co(gH)_2Py$: $C_{16}H_{17}BrCoN_5O_4$, M_r = 482.19, crystal size 0.28 × 0.20 × 0.18 mm; monoclinic; space group $P2_1/c$; a = 8.9460(15) Å, b = 26.5150(4) Å, c = 8.1980(13) Å; β = 110.657(3)°; V = 1819.6(4) Å^3; Z = 4; ρ = 1.760 Mg m^{-3}; T = 100(2) K; reflections measured/unique 11 844/4434. Final R = 0.0533 (R_w = 0.1320).

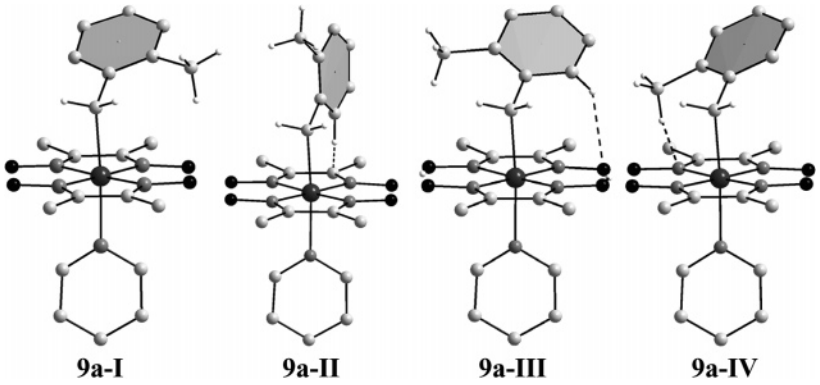

Figure 16. Calculated structures of rotational conformers of 2-Me-$C_6H_4CH_2Co(dmgH)_2Py$ (**9a**) due to C−Ph bond rotation (**9a-I**, **III**, equilibrium structures, Co1−C14−C15−C16 = +89.9/−70.1°; **9a-II**, transition state, torsion angle = +1.5°). **9a-IV** shows when 2-Me directly interacts with dioxime and the sharp increase in ΔE.

Synthesis of Organocobaloximes. $RCo(dmgH)_2Py$ (1a−11a). These compounds were synthesized by a general procedure detailed earlier for the synthesis of $RCo(dmgH)_2Py$ and involving the oxidative alkylation of Co^I with the corresponding benzyl halides.

In a typical procedure aqueous NaOH (1 pellet in 2 mL of water) was added to a suspension of $ClCo(dmgH)_2Py$ (2.02 g, 5 mmol) in methanol (30 mL). The reaction mixture was purged with argon for 20 min while cooling it to 0 °C, and a deaerated aqueous solution of sodium borohydride (0.28 g, 7.5 mmol in 1 mL of water) was added carefully to reduce Co^{III} to Co^I species. The color of the solution changed from brownish-orange to dark blue-black. An argon-purged solution of appropriate 2-substituted benzyl halide (1.5 equiv) in 1 mL of MeOH was added dropwise. The stirring was continued in the dark for another 2 h, during which the solution became orange-yellow. The reaction mixture was poured into 100 mL of ice-cold water containing a few drops of pyridine. The orange-yellow precipitate was filtered on a sintered funnel, washed with water and ether, and dried over P_2O_5 in the dark. The crude product was subjected to column chromatography.

$RCo(dpgH)_2Py$ (1b−11b). These compounds were synthesized by the same procedure as for the dmgH complexes. Also, we got a trace amount of side product (organocobalt) in some cases (**5b**, **6b**, **9b**), which could not be characterized. We could not remove this side product even after several attempts of purification (according to ^1H NMR spectra).

$RCo(gH)_2Py$ (1c−11c). These compounds were synthesized by the same procedure as that of the dmgH complexes. The yield of the gH complexes,[26b] in general, is poor, but we have been able to improve it to 65%. The problem lies mainly with the workup procedure. The gH loses its acidic proton in the basic medium of the reaction mixture, and there is no clear precipitation of the product on the addition of cold water (mixed with 2 or 3 drops of pyridine) to the reaction mixture in a standard workup procedure. Hence the product has to be extracted with chloroform. However, this forms a suspension and there is no clear separation of chloroform from the aqueous layer. Some product is lost at this stage. An addition of 4 or 5 drops of acetic acid followed by saturated NH_4Cl solution clearly separate the layers and improves the yield.

Acknowledgment. The work is supported by a grant from DST (SR/S1/IC-12/2004), New Delhi, India.

Supporting Information Available: Tables of CHN analysis data, ^{13}C NMR, and crystal data and structural refinement details; representative figures of room-temperature ^1H and ^{13}C NMR, and CIF files for X-ray crystal structures of **9a**, **11a**, **1b**, and **4c**. This material is available free of charge via the Internet at http://pubs.acs.org.

OM060940D

(40) Frisch, M. J.; Trucks, G. W.; Schlegel, H. B.; Scuseria, G. E.; Robb, M. A.; Cheeseman, J. R.; Montgomery, J. A., Jr.; Vreven, T.; Kudin, K. N.; Burant, J. C.; Millam, J. M.; Iyengar, S. S.; Tomasi, J.; Barone, V.; Mennucci, B.; Cossi, M.; Scalmani, G.; Rega, N.; Petersson, G. A.; Nakatsuji, H.; Hada, M.; Ehara, M.; Toyota, K.; Fukuda, R.; Hasegawa, J.; Ishida, M.; Nakajima, T.; Honda, Y.; Kitao, O.; Nakai, H.; Klene, M.; Li, X.; Knox, J. E.; Hratchian, H. P.; Cross, J. B.; Adamo, C.; Jaramillo, J.; Gomperts, R.; Stratmann, R. E.; Yazyev, O.; Austin, A. J.; Cammi, R.; Pomelli, C.; Ochterski, J. W.; Ayala, P. Y.; Morokuma, K.; Voth, G. A.; Salvador, P.; Dannenberg, J. J.; Zakrzewski, V. G.; Dapprich, S.; Daniels, A. D.; Strain, M. C.; Farkas, O.; Malick, D. K.; Rabuck, A. D.; Raghavachari, K.; Foresman, J. B.; Ortiz, J. V.; Cui, Q.; Baboul, A. G.; Clifford, S.; Cioslowski, J.; Stefanov, B. B.; Liu, G.; Liashenko, A.; Piskorz, P.; Komaromi, I.; Martin, R. L.; Fox, D. J.; Keith, T.; Al-Laham, M. A.; Peng, C. Y.; Nanayakkara, A.; Challacombe, M.; Gill, P. M. W.; Johnson, B.; Chen, W.; Wong, M. W.; Gonzalez, C.; Pople, J. A. *Gaussian 03*; Gaussian, Inc.: Pittsburgh, PA, 2003.

(41) Parr, R. G.; Yang, W. *Density-Functional Theory of Atoms and Molecules*; Oxford University Press: Oxford, U.K., 1989.

(42) (a) Becke, A. D. *J. Chem. Phys.* **1993**, *98*, 5648. (b) Lee, C.; Yang, W.; Parr, R. G. *Phys. Rev. B* **1998**, *37*, 785.

(43) (a) Hay, P. J.; Wadt, W. R. *J. Chem. Phys.* **1985**, *82*, 270. (b) Wadt, W. R.; Hay, P. J. *J. Chem. Phys.* **1985**, *82*, 284. (c) Hay, P. J.; Wadt, W. R. *J. Chem. Phys.* **1985**, *82*, 299. (d) Dunning, T. H., Jr.; Hay, P. J. In *Modern Theoritical Chemistry*, Schaefer, H. F., III., Ed.; Plenum: New York, 1976; pp 1−28.